[CANCER RESEARCH 64, 8643–8650, December 1, 2004]

Elevated Flk1 (Vascular Endothelial Growth Factor Receptor 2) Signaling Mediates Enhanced Angiogenesis in β_3-Integrin–Deficient Mice

Andrew R. Reynolds,[1] Louise E. Reynolds,[1] Tobi E. Nagel,[2] Julie C. Lively,[3] Stephen D. Robinson,[1] Daniel J. Hicklin,[4] Sarah C. Bodary,[5] and Kairbaan M. Hodivala-Dilke[1]

[1]Cell Adhesion and Disease Group, Tumour Biology Laboratory, Cancer Research UK Clinical Centre, Barts and the London, Queen Mary's School of Medicine and Dentistry, John Vane Science Centre, London, United Kingdom; [2]Genentech, Inc., South San Francisco, California; [3]Center for Matrix Biology, Department of Medicine, Beth Israel Deaconess Medical Center and Harvard Medical School, Boston, Massachusetts; [4]ImClone Systems, Inc., New York, New York; and [5]DNAX, Palo Alto, California

ABSTRACT

Tumor growth, tumor angiogenesis, and vascular endothelial growth factor (VEGF)–specific angiogenesis are all enhanced in β_3-integrin–null mice. Furthermore, endothelial cells isolated from β_3-null mice show elevated levels of Flk1 (VEGF receptor 2) expression, suggesting that β_3-integrin can control the amplitude of VEGF responses by controlling Flk1 levels or activity. We now show that Flk1 signaling is required for the enhanced tumor growth and angiogenesis seen in β_3-null mice. Moreover, β_3-null endothelial cells exhibit enhanced migration and proliferation in response to VEGF *in vitro*, and this phenotype requires Flk1 signaling. Upon VEGF stimulation, β_3-null endothelial cells exhibit higher levels of phosphorylated Flk1 and extracellular-related kinases 1 and 2 than wild-type endothelial cells. Furthermore, signaling via ERK1/2 is required to mediate the elevated responses to VEGF observed in β_3-null endothelial cells and aortic rings *in vitro*. These data confirm that VEGF signaling via Flk1 is enhanced in β_3-integrin–deficient mice and suggests that this increase may mediate the enhanced angiogenesis and tumor growth observed in these mice *in vivo*.

INTRODUCTION

A favorable shift in the local concentrations of pro- and anti-angiogenic mediators is required for tumor neovascularization to occur (1). The expression of $\alpha_v\beta_3$ and $\alpha_v\beta_5$ integrin on endothelial cells has long been considered a pro-angiogenic event, because their expression is up-regulated on newly formed vessels (2, 3); whereas antagonists of $\alpha_v\beta_3$ and $\alpha_v\beta_5$ have been shown to inhibit pathological angiogenesis and tumor growth in animal models (2–5). Furthermore, the β_3-integrin antagonist, Vitaxin, is currently in clinical trials (6). However, we demonstrated recently that pathologic angiogenesis and tumor growth are actually enhanced in β_3-integrin–deficient or β_3/β_5-integrin doubly-deficient mice (7); these findings have brought into question the role of β_3-integrin as a positive regulator of angiogenesis (7, 8). Instead, we showed that the enhanced angiogenesis may be due to an elevated response to vascular endothelial growth factor (VEGF) in these mice. Because both VEGF and β_3-integrin signaling are prominent targets of anti-angiogenic therapy (9), the mechanism via which this enhanced response occurs requires additional investigation.

VEGF initiates tumor vascularization by driving an angiogenic response in endothelial cells (1, 10–12). VEGF-A, the principal isoform of VEGF implicated in this process, mediates its effects via at least two receptor tyrosine kinases expressed on endothelial cells, VEGF receptor 1 (VEGFR1/Flt1) and VEGF receptor 2 (VEGFR2/Flk1), and a coreceptor, neuropilin-1 (10, 12). Most reports agree that Flk1 activation is necessary and sufficient for angiogenic responses to VEGF-A (10, 12–14). However, Flt1 can have either a positive or negative effect on Flk1 signaling (12, 15–17), whereas neuropilin-1 can enhance signaling through Flk1, but can inhibit angiogenesis by binding to semaphorin ligands (18–21).

Tyrosine phosphorylation of Flk1 in response to VEGF activates numerous downstream signaling molecules, including the extracellular-related kinases 1 and 2 (ERK1/2). ERK1/2 activity is a known mediator of endothelial cell proliferation, migration, and survival during angiogenesis (22–24). Furthermore, Flk1 expression is up-regulated on new blood vessels (25–27) and antagonists that block the function of VEGF-A or Flk1 inhibit tumor growth and angiogenesis in mice (9, 28–32). Thus the level of Flk1 expression and the signaling activity of this receptor are considered to be of central importance to VEGF-specific angiogenesis.

Endothelial cells isolated from β_3-null mice show elevated expression levels of Flk1. We proposed that these raised levels of Flk1 expression might facilitate an enhanced response to VEGF in β_3-null endothelial cells (7), explaining the enhanced tumor and VEGF-specific angiogenesis observed in these mice. In the current report, we have used specific inhibitors of Flk1 to investigate this hypothesis *in vivo* and *in vitro*. We show that not only are the enhanced angiogenesis and tumor growth observed in β_3-null mice dependent on VEGF binding to Flk1 *in vivo*, but that β_3-null endothelial cells show enhanced Flk1-dependent responses to VEGF *in vitro*. Furthermore, enhanced responses to VEGF in β_3-null endothelial cells requires ERK1/2 signaling. These results have important implications for the current understanding of how $\alpha_v\beta_3$ integrin regulates VEGF signaling and tumor angiogenesis.

MATERIALS AND METHODS

Materials. All chemicals and reagents were from Sigma (Poole, United Kingdom), except for the following: DC101 rat monoclonal anti-Flk1 antibody and rat immunoglobulin G (IgG) control antibody (ImClone Systems, Inc., New York, NY), anti-ERK1, anti-ERK2, anti-HSC-70 (Autogen Bioclear, Oxfordshire, United Kingdom), anti-phospho-ERK1/2 (Cell Signaling Technology, Hitchin, United Kingdom), anti-Fcγ III/II receptor, anti-Flk1, anti-CD31, anti-ICAM-2 (BD PharMingen, Oxford, United Kingdom), anti-Flk1-pY1173–specific antibody (Oncogene Research Products, San Diego, CA), anti-laminin-1 (Sigma), growth factor reduced–Matrigel (GFR-Matrigel; BD Biosciences, Oxford, United Kingdom), VEGF-A^{164} (R&D Systems, Oxford, United Kingdom or Peprotech, London, United Kingdom), interferon-γ (IFN-γ; R&D Systems), endothelial cell growth mitogen (Biogenesis, Poole, United Kingdom), fetal calf serum (Biowest, Miami, FL), SU5416, UO126, fibronectin (Calbiochem, Beeston, United Kingdom), Vitrogen (ICN Biosciences, Irvine, CA), Ham's F-12, and Dulbecco's modified Eagle's medium (DMEM; Cancer Research UK).

Mouse Tumor Models. The B16F0 cell line used in these studies is a nonmetastatic variant of the B16 melanoma cell line (33). The CMT19T cell line is a mouse lung carcinoma cell line derived from the CMT167 cell line (34). Subcutaneous tumors were grown in age- and sex-matched wild-type or β_3-integrin–deficient mice on a mixed genetic background (C57BL6/129Sv). Two days before injection of tumor cells (day 0), wild-type and β_3-null mice received an intraperitoneal injection of DC101 antibody (800 μg in 100 μL of

Received 8/2/04; revised 9/20/04; accepted 9/29/04.

The costs of publication of this article were defrayed in part by the payment of page charges. This article must therefore be hereby marked *advertisement* in accordance with 18 U.S.C. Section 1734 solely to indicate this fact.

Requests for reprints: Kairbaan M. Hodivala-Dilke, Cell Adhesion and Disease Group, Tumour Biology Laboratory, Cancer Research UK Clinical Centre, Barts and the London, Queen Mary's School of Medicine and Dentistry, John Vane Science Centre, Charterhouse Square, London EC1M 6BQ, United Kingdom. Phone: 44-207-014-0406; Fax: 44-207-014-0401; E-mail: Kairbaan.Hodivala-Dilke@cancer.org.uk.

PBS) or PBS vehicle control. This dose of DC101 has been shown previously to be the maximum effective dose in mice (28) and was selected to block all Flk1 receptor activity. Tumors were established by subcutaneous injection of 1×10^6 B16F0 or CMT19T cells between the shoulders of wild-type and β_3-null animals on day 2. All animals received additional DC101 or PBS/IgG control injections on days 2, 5, and 8. Tumors were harvested on day 12 and photographed, and tumor volume was measured. Similar results were obtained in tumor assays regardless of whether we used a PBS vehicle or isotype-matched IgG as the control injection.

Quantification of Blood Vessel Density in Tumor Sections. Size-matched tumors from wild-type and β_3-integrin–null mice treated with or without Flk1 inhibitor were snap-frozen and bisected, and cryosections were made. Frozen sections were brought to room temperature, fixed in 100% acetone at −20°C, rehydrated in PBS for 10 minutes, and then blocked (PBS, 1% bovine serum albumin, and 1:60 normal goat serum) for 45 minutes at room temperature. After a 5-minute wash in PBS, sections were incubated with 1:100 anti-laminin-1 or 1:100 anti-CD31 antibody in blocking buffer for 2 hours at room temperature. After three 5-minute washes in PBS, sections were incubated with Alexa 488-antirabbit or Alexa 488-antirat secondary antibody (Molecular Probes, Eugene, OR) diluted in blocking buffer. After three 5-minute washes in PBS, sections were washed briefly with distilled water before being mounted in mounting medium with antifade (Citifluor, Ltd., Leicester, United Kingdom). Immunofluorescence images were captured using an epifluorescence microscope (Carl Zeiss, Jena, Germany) equipped with a digital camera (Hamamatsu Photonics, Ltd., Welwyn Garden City, United Kingdom) using Open Lab v2.2 software (Improvision, Coventry, United Kingdom). The number of laminin-1– or CD31-positive blood vessels present across the entire area of each tumor section was counted and divided by the area of the section to determine tumor blood vessel density.

***In vivo* Matrigel Plug Assay.** Matrigel plug assays were performed in age- and sex-matched wild-type or β_3-integrin–deficient mice. On day 0, animals received an intraperitoneal injection of DC101 or IgG control antibody (800 μg in 100 μL of PBS). On day 2, each animal received an abdominal subcutaneous injection in the left and right flank containing 200 μL of GFR-Matrigel mixed with 30 ng of VEGF. Animals received additional DC101 or IgG control injections on days 2, 5, and 8. Matrigel plugs were removed on day 9, fixed in formal saline, bisected, embedded in paraffin, and sectioned. Sections were stained with hematoxylin and eosin for analysis of blood vessel infiltration. Images of histological sections were captured using the microscope described above. The number of blood vessels present across the entire area of each Matrigel section was counted and divided by the area of the section to determine blood vessel density.

***Ex vivo* Aortic Ring Assay.** Thoracic aortae were removed from 6- to 9-week-old wild-type or β_3-integrin–deficient mice after cervical dislocation. Extraneous fat and other tissue was removed, and the aortae were sliced transversely into ~0.5-mm-thick rings. Each ring was transferred to a 50 μL bed of polymerized GFR-Matrigel. An additional 50 μL of GFR-Matrigel were then applied over the ring and allowed to polymerize before adding 150 μL of basal medium: DMEM with 2% fetal calf serum (FCS). The medium was supplemented further with 30 ng/mL VEGF and inhibitors or antibodies as appropriate. Where antibodies were used, the GFR-Matrigel was supplemented with 20 μg/mL DC101 antibody or control IgG just before polymerization. This dose of anti-VEGFR2 antibody has been shown previously to be the maximum effective dose within several *in vitro* assays (35) and was selected to block all Flk1 receptor activity. Aortic rings were cultured at 37°C for 8 days. Every 2 days, the medium including growth factors, inhibitors, or antibodies, if added, was replaced. On day 6, phase contrast photomicrographs of rings were taken using an inverted microscope (Carl Zeiss) equipped with a digital camera (Hamamatsu Photonics, Ltd.), and angiogenesis was quantitated by counting the numbers of capillary sprouts per ring.

Isolation and Culture of Mouse Lung Endothelial Cells. Primary mouse lung endothelial cells were isolated from the lungs of wild-type and β_3-integrin–deficient mice on a 129Sv background, whereas temperature-conditional immortalized endothelial cells were isolated from the lungs of animals crossed with H-2K^b-tsA58 "immorto" mice, which express a temperature-sensitive simian virus 40 large T-antigen (36). Lungs were minced, digested with collagenase type I (Gibco Invitrogen, Ltd., Paisley, United Kingdom), and sieved through a 70 μm-pore size cell strainer (BD Falcon, Bedford, MA); and the cell suspension was plated on flasks precoated with 0.1% gelatin, 10 μg/mL fibronectin, and 30 μg/mL Vitrogen in PBS. Endothelial cells were purified by magnetic immunosorting with a single negative sort for Fcg III/II receptor–positive macrophages and at least two positive sorts for ICAM-2–positive endothelial cells. Cells were cultured routinely in a 50:50 mix of Ham's F-12:DMEM medium supplemented with 20% FCS, 20 μg/mL endothelial cell mitogen, 1 μg/mL heparin, and antibiotics in flasks precoated as described above. Temperature-conditional immortalized mouse lung endothelial cells were cultured at 33°C in medium supplemented with 20 U/mL IFN-γ to permit simian virus 40 T-antigen activity and switched to 37°C in the absence of IFN-γ 24 hours before use in experiments, to prevent T-antigen activity and therefore render the endothelial cells with a primary phenotype (37).

Migration Assays. Temperature-conditional immortalized mouse lung endothelial cells were plated at a density of 10,000 cells per square centimeter in precoated six-well plates. Cells were grown until a confluent monolayer was achieved, and then the medium was exchanged for serum-free medium supplemented with inhibitors, DC101 antibody, or control IgG as appropriate. After 1 hour, monolayers were scratched with a P-200 tip, and the scratches were photographed at three to five points along their length using the inverted microscope described above. The medium was then exchanged for a 50:50 mix of Ham's F-12:DMEM supplemented with VEGF and inhibitors or antibodies as appropriate. After 8 hours of incubation at 37°C, scratches were rephotographed, and the percentage of migration was determined relative to the scratch width at 0 hours.

Proliferation Assays. Primary mouse lung endothelial cells were plated at a density of 2500 cells per square centimeter in precoated six-well plates. Twenty-four hours later, the medium was changed for a 50:50 mix of Ham's F-12:DMEM supplemented with 1% FCS, 1 mg/mL heparin, and 50 ng/mL VEGF with or without 3 μmol/L SU5416, a Flk1 tyrosine kinase inhibitor (Calbiochem). This dose of SU5416 has been shown previously to be the maximum effective dose within several *in vitro* assays (32, 38) and was selected to block all Flk1 receptor activity. Cells were trypsinized from replicate wells every day for five days and counted using a hemocytometer.

Western Blotting and Immunoprecipitation. Wild-type or β_3-null temperature-conditional immortalized mouse lung endothelial cells were plated at a density of 5,000 cells per square centimeter in 6- or 10-cm-diameter precoated dishes and grown to 70 to 90% confluency. The medium was then exchanged for serum-free medium for 3 hours with addition of inhibitors or antibodies as appropriate during the last hour of serum starvation, after which cells were stimulated with 10 ng/mL VEGF. Stimulation was terminated by transfer of the cells to ice, followed by washing three times with ice-cold PBS and lysis in ice-cold lysis buffer: 10 mmol/L Tris (pH 7.3), 150 mmol/L NaCl, 10 mmol/L EGTA, 1% Triton X-100, 1% sodium deoxycholate, 0.1% SDS, 5 mmol/L NaF, 1 mmol/L Na_3VO_4, 1 mmol/L phenylmethylsulfonyl fluoride, and protease inhibitor cocktail (Calbiochem). Cells were then incubated for an additional 10 minutes on ice before scraping the cells off and pelleting insoluble material at 12,000 rpm for 10 minutes.

Alternatively, for immunoprecipitation of phosphorylated Flk1, serum-starved cells were preincubated for 10 minutes with serum-free medium containing 1 mmol/L Na_3VO_4 and 1 μg/mL heparin, followed by stimulation with 50 ng/mL VEGF in the same medium for 7 minutes at 37°C. Cells were then transferred to ice, washed with ice-cold PBS plus 1 mmol/L Na_3VO_4, and lysed for 15 minutes in immunoprecipitation buffer: 20 mmol/L Tris (pH 7.5), 150 mmol/L NaCl, 1 mmol/L Na_3VO_4, 1% NP40, 10% glycerol, and protease inhibitor cocktail, before scraping the cells off and pelleting insoluble material at 12,000 rpm for 10 minutes. The supernatants were incubated with 5 μg of anti-Flk1 antibody overnight at 4°C with end-over-end rotation, followed by an additional 2 hours of incubation with protein A/G Sepharose beads (Autogen Bioclear). The beads were then washed three times with lysis buffer before boiling in SDS-PAGE sample loading buffer.

Lysates were subjected to SDS-PAGE and transferred to nitrocellulose membranes (Hybond ECL; Amersham Biosciences, Buckinghamshire, United Kingdom) for Western blotting with antiphosphorylation site-specific antibodies, followed by stripping and reprobing with anti-ERK1/2 or anti-Flk1 antibodies. Blots were probed for HSC-70 to determine the equality of protein loading. Densitometry was performed using a gel acquisition and analysis set-up (UV Products, Ltd., Cambridge, United Kingdom). Band densities were normalized to HSC-70 levels to make quantitative measurements of protein phosphorylation and total protein levels.

Analysis of Statistical Significance. Data sets were analyzed for significance using Student's *t* test. $P < 0.05$ was considered statistically significant.

RESULTS

Flk1 Antagonist Blocks Enhanced Tumor Growth in β_3-Null Mice. To address the role that Flk1 plays in the enhanced angiogenesis observed in β_3-null mice *in vivo* we used an antibody, DC101, which is raised against the extracellular domain of Flk1 and antagonizes VEGF binding to the receptor. This Flk1 inhibitor has been shown to block both tumor growth and angiogenesis in several mouse models (28–30). B16F0 melanomas grown in β_3-null control mice were significantly larger than those found in wild-type control mice ($P < 0.05$; Fig. 1*A* and *B*), in agreement with our previous findings (7). However, there was a significant reduction in tumor volume in both wild-type and β_3-null animals treated with Flk1 inhibitor, when compared with control animals of the same genotype ($P < 0.05$; Fig. 1*A* and *B*). The same type of experiment was performed using the mouse carcinoma cell line, CMT19T. Again, tumors grown subcutaneously in β_3-null animals were significantly larger than those harvested from wild-type mice ($P < 0.03$ Fig. 1*C* and *D*), and administration of Flk1 inhibitor resulted in a significant reduction in tumor volume in both genotypes ($P < 0.03$; Fig. 1*C* and *D*). Importantly, in the presence of the Flk1 inhibitor, there was no significant difference in the size of tumors observed in β_3-null and wild-type mice ($P > 0.05$; Fig. 1). Because neither tumor cell line used in this study expresses Flk1 (data not shown), it is unlikely that the effect of the Flk1 inhibitor is due to direct toxicity against the tumor cells. Moreover, these data suggest that the enhanced tumor volume observed in β_3-integrin–deficient mice can be blocked by inhibiting Flk1 on angiogenic blood vessels.

Flk1 Antagonist Blocks Enhanced Angiogenesis in β_3-Null Mice. To confirm the role played by Flk1 in β_3-null angiogenic blood vessels, we evaluated the effect that Flk1 inhibition has on tumor angiogenesis in β_3-null mice. Size-matched tumors removed from wild-type and β_3-null animals, treated with and without Flk1 inhibitor, were processed for histological examination. Blood vessel densities in tumors were determined by performing immunohistochemistry for laminin-1 (Fig. 2*A*) or CD31 (data not shown) and counting the number of blood vessels present across entire tumor sections. The blood vessel density in tumors from β_3-null mice was significantly higher than in tumors from wild-type mice ($P < 0.007$; Fig. 2*B*). However, in the presence of the Flk1 inhibitor, blood vessel densities were significantly lower than in untreated animals ($P < 0.007$; Fig. 2*B*), and there was no significant difference in blood vessel density between genotypes (Fig. 2*B*). Sections stained for CD31 gave identical results (data not shown). These results show that the enhanced tumor angiogenesis observed in β_3-null mice can be inhibited using a Flk1 antagonist.

To confirm the role of Flk1 in an independent *in vivo* assay of angiogenesis, wild-type and β_3-null mice were implanted with VEGF-containing Matrigel plugs (7). The mice were treated with or without a course of Flk1 inhibitor, and the density of blood vessel infiltration into the plugs was determined by histology (Fig. 2*C* and *D*). The vessel density in plugs removed from β_3-null mice was significantly higher than that found in plugs from wild-type mice ($P < 0.0005$; Fig. 2*D*). However, in the presence of the Flk1 inhibitor, vessel densities were significantly lower than in untreated animals ($P < 0.0004$; Fig. 2*D*), and there was no significant difference in vessel density between genotypes.

Finally, we confirmed that similar results could be obtained in the *ex vivo* aortic ring assay (7). Aortic ring segments from wild-type and β_3-null mice were embedded in Matrigel and stimulated with or without VEGF in the presence of Flk1 inhibitor or IgG control antibody. Angiogenesis was quantified by counting the number of microvessels that sprouted directly from the rings (Fig. 3*A*). VEGF-dependent sprouting of β_3-null rings was enhanced when compared with rings without VEGF ($P < 0.0003$; Fig. 3*B*) and when compared with wild-type rings incubated with VEGF ($P < 0.0003$; Fig. 3*B*).

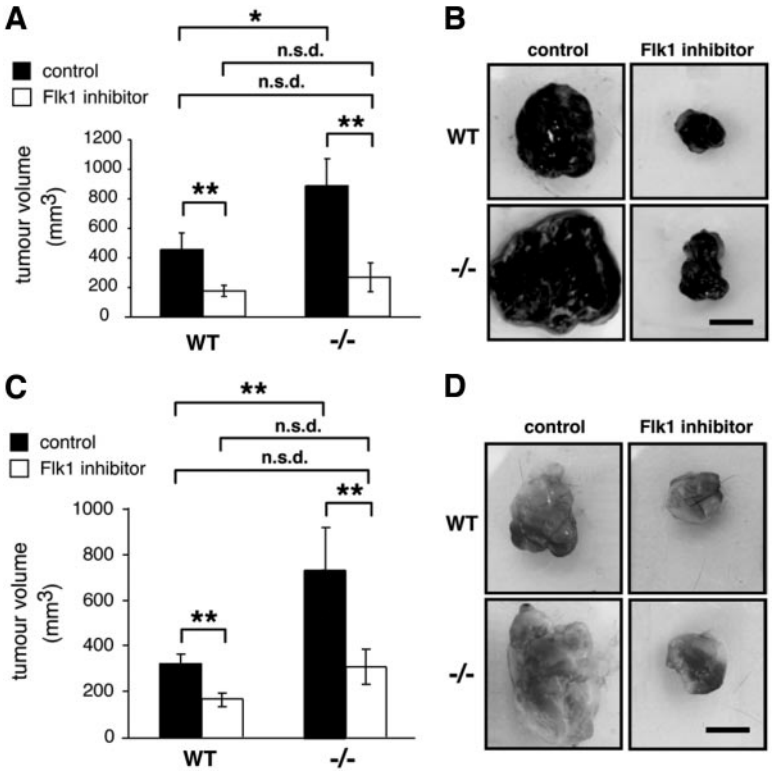

Fig. 1. Flk1 inhibitor blocks enhanced tumor growth in β_3-integrin–deficient mice. Mice received intraperitoneal injections of a Flk1 inhibitory antibody, DC101 (800 μg in 100 μL of PBS), or control 2 days before subcutaneous injection of 1×10^6 B16F0 melanoma cells or 1×10^6 CMT19T mouse carcinoma cells. Additional intraperitoneal injections of Flk1 inhibitor or control were carried out on the day of tumor cell injection and every 3 days after. Tumors were removed 10 days after injection of cells, size measured, and photographed. *A*, quantification of subcutaneous B16F0 melanoma tumor volume in wild-type (*WT*) and β_3-null (−/−) animals treated with Flk1 inhibitor or control; $n = 10$ animals per data point; *, $P < 0.05$; **, $P < 0.03$; n.s.d., no significant difference. *B,* photographs of representative B16 melanomas. *C*, quantification of subcutaneous CMT19T tumor volume in wild-type and β_3-null animals treated with Flk1 inhibitor or control; $n = 5$ animals per data point; **, $P < 0.03$; n.s.d., no significant difference. *D,* photographs of representative CMT19T tumors. *Bars* show mean tumor volume in cubic millimeters ± *SEM*. *Scale bar* = 5 mm.

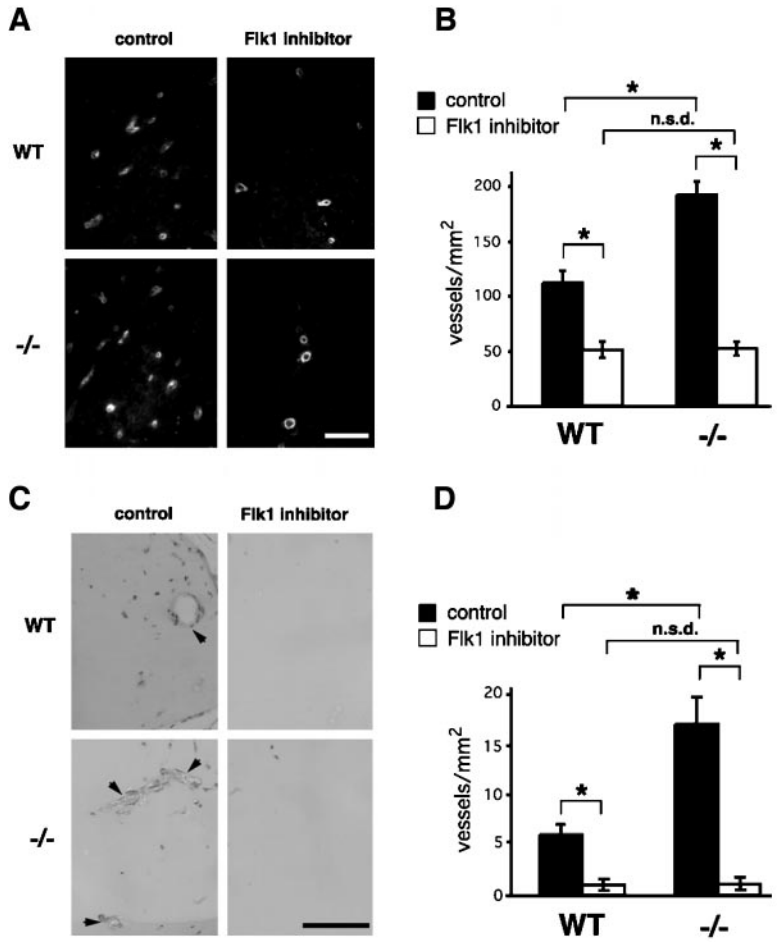

Fig. 2. Flk1 inhibitor blocks enhanced angiogenesis in β_3-integrin–deficient mice. Mice received intraperitoneal injections of Flk1 inhibitor (800 μg in 100 μL PBS) or control 2 days before subcutaneous injection of 1×10^6 B16F0 melanoma cells or subcutaneous injection of Matrigel plugs (200 μL of Matrigel plus 30 ng of VEGF per plug). Additional intraperitoneal injections of Flk1 inhibitor or control were carried out on the day of tumor or Matrigel injection and every 3 days after. *A* and *B*. Melanomas were removed 10 days after tumor cell injection and snap-frozen. Tumor blood vessels were identified in cryosections from size-matched tumors by immunofluorescence staining for laminin-1 or CD31. *A,* representative images of laminin-1 staining in tumor sections. *B,* quantification of tumor blood vessel density (three tumors per data point); *, $P < 0.007$; n.s.d., no significant difference. *C* and *D*. Matrigel plugs were removed 7 days after their injection, fixed in formalin, and embedded in paraffin; and sections were stained with hematoxylin and eosin. *C*, representative images of Matrigel plug sections stained with hematoxylin and eosin; *arrowheads* indicate blood vessels. *D*, quantification of blood vessel densities in Matrigel plugs (15–20 plugs per data point); *, $P < 0.0005$; n.s.d., no significant difference. *Bars* show the mean vessel number per square millimeter ± *SEM*. *Scale bar* = 100 μm. *WT*, wild-type; −/−, β_3-null.

Furthermore, sprouting from β_3-null rings was inhibited significantly by the presence of Flk1 inhibitor ($P < 0.0003$; Fig. 3*B*) and was equivalent to sprouting seen in the absence of VEGF or in wild-type rings. Interestingly, we observed no increased stimulation of sprouting in wild-type rings when VEGF was added. This observation highlights the impact that β_3-integrin–deficiency has on VEGF-specific angiogenesis.

Therefore, within three independent assays of angiogenesis, blockade of Flk1 function inhibited the enhanced angiogenesis in β_3-null mice.

Inhibition of Flk1 Blocks Enhanced Vascular Endothelial Growth Factor-Mediated Migration and Proliferation of β_3-Null Endothelial Cells. Migration and proliferation of endothelial cells are both required for *de novo* blood vessel formation (1). Because VEGF stimulates enhanced angiogenesis in β_3-null mice through Flk1, we investigated whether β_3-null endothelial cells exhibit enhanced migratory or proliferative responses to VEGF *in vitro* using endothelial cells isolated from the lungs of wild-type and β_3-null mice.

Endothelial cell migration was assayed by measuring the extent of closure during *in vitro* scratch assays (Fig. 4*A* and *B*). In the absence of growth factors, migration of wild-type and β_3-null endothelial cells was equivalent. VEGF stimulated a significant increase in wild-type endothelial cell migration when compared with growth factor–free medium ($P < 0.05$; Fig. 4*B*), but β_3-null endothelial cells migrated significantly further than wild-type cells in response to VEGF ($P < 0.005$; Fig. 4*B*). Furthermore, the Flk1 inhibitor reduced the VEGF-dependent migration of both wild-type and β_3-null endothelial cells down to levels seen in growth factor-free medium. Importantly, for both wild-type and β_3-null cells, the Flk1 inhibitor had no effect on basal migration levels or on migration induced by incubating cells with 10% FCS (data not shown), indicating that the Flk1 inhibitor acts specifically to block VEGF-mediated responses.

Endothelial cell proliferation in response to VEGF was assayed by incubating cells with VEGF in the presence of 1% serum and counting the number of cells every day for 5 days. Although these conditions supported the survival of wild-type endothelial cells, no increase in cell number was evident (Fig. 4*C*). In contrast, VEGF stimulated the proliferation of β_3-null endothelial cells. Within 3 days of beginning the experiment, the number of β_3-null cells measured was significantly greater than the number of wild-type cells ($P < 0.001$); and by 5 days, the number of β_3-null endothelial cells was 4- to 6-fold greater than the number of wild-type cells ($P < 0.0004$). Furthermore, application of SU5416, a Flk1 tyrosine kinase inhibitor (32), significantly attenuated the VEGF-dependent proliferation of β_3-null endothelial cells ($P < 0.001$ at 3–5 days) but had little effect on the numbers of wild-type cells recorded. Importantly, both wild-type and β_3-null endothelial cells proliferated in normal growth medium, containing 20% FCS and endothelial mitogen, and this was not affected by the Flk1 inhibitor (data not shown). Taken together, these data demonstrate that β_3-null endothelial cells show both enhanced migration and proliferation in response to VEGF when compared with wild-type cells and that inhibition of Flk1, using two independent Flk1 inhibitors, blocks these responses.

Enhanced Phosphorylation of Flk1 and Extracellular-Related Kinase 1/2 in β_3-Null Endothelial Cells. Given that VEGF-stimulated responses are enhanced in β_3-null endothelial cells, we investigated whether intracellular signaling in response to VEGF also is

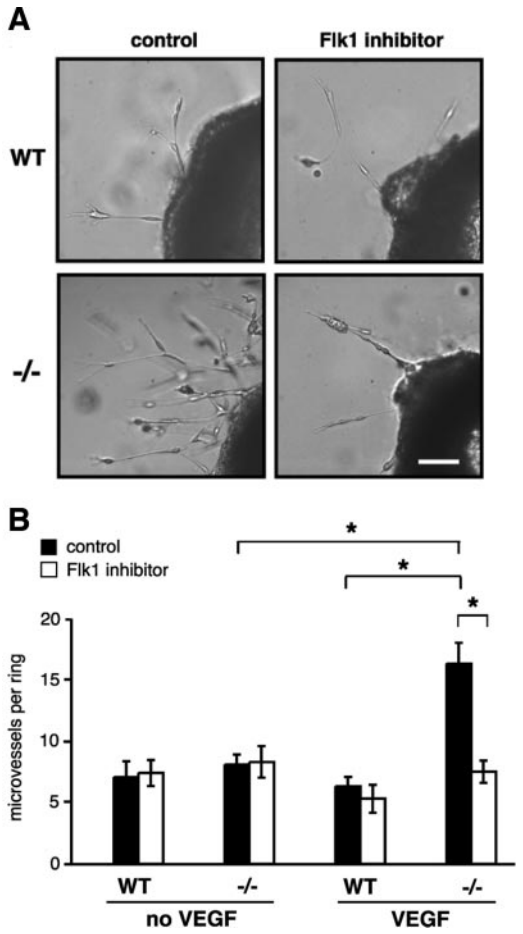

Fig. 3. Enhanced sprouting angiogenesis from β_3-integrin–deficient aortic rings in response to VEGF is blocked by Flk1 inhibitor. *A* and *B*, aortic rings from wild-type (*WT*) and β_3-null (−/−) mice were embedded in Matrigel and overlaid with medium. Cultures were supplemented with or without 30 ng/mL VEGF in the presence of antibodies (20 μg/mL DC101 or 20 μg/mL control IgG) and incubated for 8 days at 37°C with replacement of the medium every 2 days. *A*, representative photomicrographs of VEGF-stimulated aortic rings after 6 days in culture. *B*, sprouting angiogenesis was quantified by counting the number of microvessels that developed from aortic rings after 6 days in culture ($n = 15$ rings per data point); *, $P < 0.0003$. *Bars* show mean microvessel number per ring ± *SEM*. *Scale bar* = 100 μm.

enhanced. We have shown previously that β_3-null endothelial cells express 2- to 3-fold more Flk1 than wild-type endothelial cells (7). Therefore, we examined whether VEGF stimulation of β_3-null endothelial cells results in increased levels of phosphorylated Flk1. VEGF stimulated the phosphorylation of Flk1 in both wild-type and β_3-null endothelial cells (Fig. 5*A*). Furthermore, densitometric analysis of Western blots revealed that the levels of phosphorylated Flk1 induced by VEGF were approximately 2-fold elevated in β_3-null endothelial cells when compared with wild-type cells (Fig. 5*B*). Densitometric analysis of total Flk1 levels confirmed that total Flk1 levels were also 2-fold elevated in β_3-null cells in this experiment (Fig. 5*C*). This confirms that, upon VEGF stimulation, β_3-null endothelial cells have elevated levels of phosphorylated Flk1 when compared with wild-type cells.

To investigate whether elevated levels of phosphorylated Flk1 in β_3-null cells can be translated into an enhanced downstream signaling response, we investigated the phosphorylation of ERK1/2 in response to VEGF. Several reports have shown that VEGF signaling through Flk1 activates ERK1/2 phosphorylation and that this is required for migration and proliferation of endothelial cells *in vitro* (10, 12). VEGF stimulated the phosphorylation of ERK1/2 in both wild-type and β_3-null endothelial cells (Fig. 5*D* and *E*). This response peaked at 5 minutes after stimulation and was down-regulated to basal levels in both cell types by 15 minutes (Fig. 5*D* and *E*). However, the levels of phosphorylated ERK1/2 detected in β_3-null endothelial cells after VEGF stimulus were consistently higher than those detected in wild-type cells (Fig. 5*D* and *E*). ERK1/2 phosphorylation was blocked by application of the MEK1 inhibitor PD 098059 (Fig. 5*F* and *G*), indicating that the signaling from Flk1 to ERK1/2 occurred via activation of MEK1. Impor-

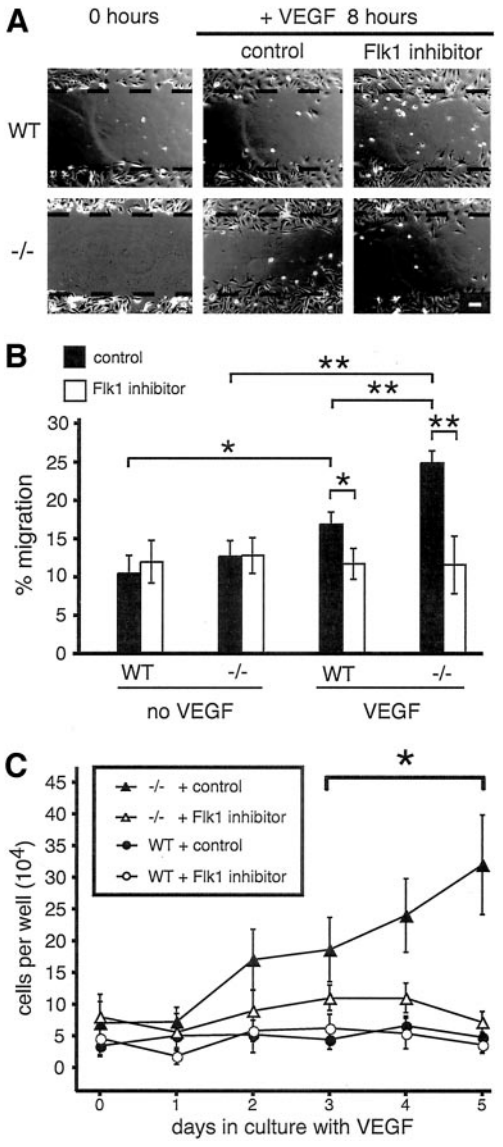

Fig. 4. Enhanced migration and proliferation of β_3-null endothelial cells in response to VEGF are blocked by Flk1 inhibitors. *A* and *B*. Wild-type (*WT*) or β_3-null (−/−) endothelial cells were grown to confluency in six-well plates. After preincubation with serum-free medium plus antibodies (20 μg/mL DC101 or 20 μg/mL control IgG), monolayers were scratched with a P-200 pipette tip. Cells were then incubated for 8 hours with serum-free medium or medium plus 25 ng/mL VEGF with or without antibodies (20 μg/mL DC101 or 20 μg/mL control IgG). *A,* representative photomicrograph images of wild-type and β_3-null endothelial cell scratches at 0 hours and after 8 hours of migration under different stimulation conditions. *B,* quantification of percentage migration displayed by wild-type and β_3-null endothelial cells under different stimulation conditions; *, $P < 0.05$; **, $P < 0.005$. *Bars* show percentage migration relative to 0 hours ± *SEM*. *Scale bar* = 100 μm. *C*. Wild-type and β_3-null endothelial cells were seeded at a density of 2500 cells per square centimeter in six-well plates. After 24 hours, the medium was exchanged for that containing 1% FCS and 50 ng/mL VEGF with 3 μmol/L SU5416 or vehicle control (day 0). Cells from representative wells were trypsinized and counted every subsequent day for 5 days (days 1–5). Each data point represents the mean from five counts, and *bars* show cell number ± *SEM*; *, $P < 0.001$ when comparing significant difference between number of wild-type and β_3-null cells recorded in the presence of VEGF without Flk1 inhibitor.

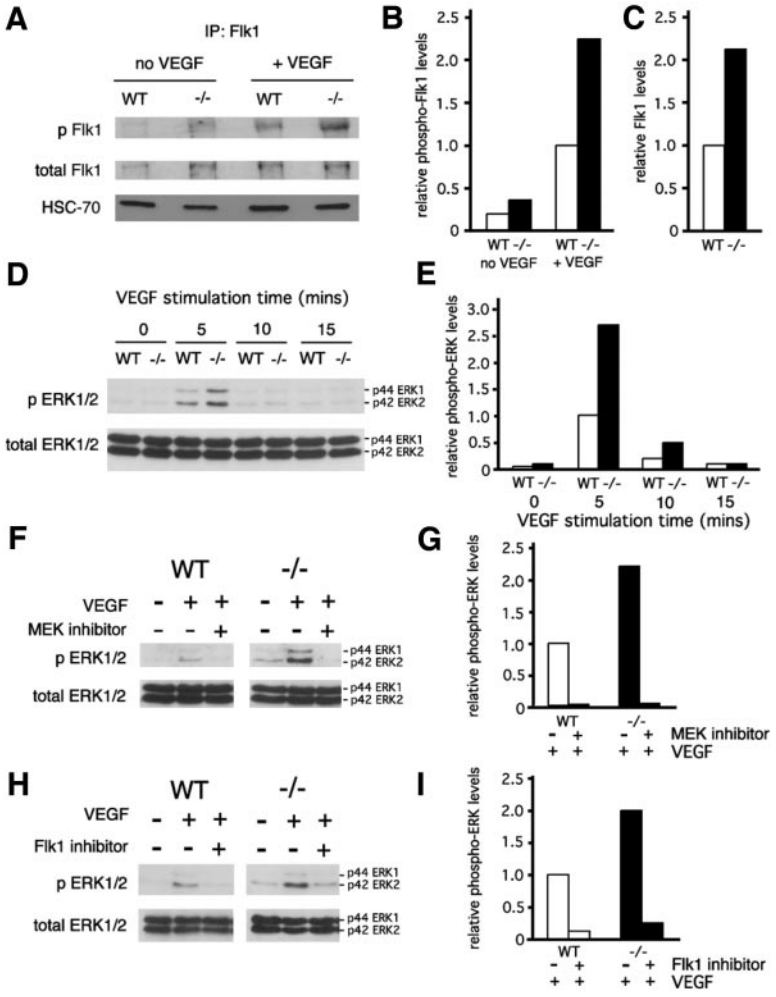

Fig. 5. Enhanced VEGF-mediated signaling in β_3-null endothelial cells. *A*. Subconfluent wild-type (*WT*) or β_3-null (−/−) endothelial cells were serum-starved and then stimulated with 50 ng/mL VEGF for 7 minutes and then lysed. Flk1 was immunoprecipitated from lysates and detected by probing Western blots for phospho-Flk1 (*p Flk1*) and then stripping and reprobing for Flk1 (*total Flk1*). The Western blot for HSC-70 was performed on a parallel Western blot that was loaded with the same proportions of lysate as used for each immunoprecipitation. *B*, densitometric quantification of Flk1 phosphorylation levels in wild-type and β_3-null endothelial cells in response to VEGF. *C*, densitometric quantification of Flk1 total protein levels in wild-type and β_3-null endothelial cells. *D*, phosphorylation of ERK1/2 (*p ERK1/2*) in wild-type and β_3-null endothelial cells in response to VEGF. *E*, densitometric quantification of ERK1/2 phosphorylation in wild-type and β_3-null endothelial cells in response to VEGF. *F*, ERK1/2 phosphorylation in wild-type and β_3-null endothelial cells in response to a 5-minute treatment with VEGF in the presence or absence of 5 μmol/L PD 098059 (*MEK1 inhibitor*). *G,* densitometric quantification of ERK1/2 phosphorylation in wild-type and β_3-null endothelial cells in response to VEGF with and without pretreatment with 5 μmol/L PD 098059. *H*, phosphorylation of ERK1/2 after 1 hour of preincubation with or without Flk1 inhibitor (20 μg/mL) and 5 minutes of stimulation with VEGF. *I,* densitometric quantification of ERK1/2 phosphorylation in wild-type and β_3-null endothelial cells in response to VEGF with and without pretreatment with Flk1 inhibitor (20 μg/mL). Densitometry results in parts *B*, *C*, *E*, *G*, and *I* are normalized to an HSC-70 loading control. The data are representative of results obtained in three independent experiments.

tantly, phosphorylation of ERK1/2 was ablated in both wild-type and β_3-null cells when VEGF stimulation was performed in the presence of Flk1 inhibitor, indicating that this response also depended on signaling through Flk1 (Fig. 5*H* and *I*). These data show that VEGF stimulation results in elevated levels of phosphorylated Flk1 in β_3-null endothelial cells and that this is associated with enhanced activation of ERK1/2 via MEK1.

Responses to Vascular Endothelial Growth Factor in Wild-Type and β_3-Null Endothelial Cells Involve Signaling via Extracellular-Related Kinase 1/2. Finally, we investigated whether the activation of ERK1/2 is involved in the enhanced response of β_3-null endothelial cells to VEGF. The MEK1/2 inhibitor UO126 inhibited VEGF-stimulated migration of both wild-type and β_3-null endothelial cells in a dose-dependent fashion (Fig. 6*A*). Furthermore, at the nonsaturating doses of 0.05 and 0.1 μmol/L, with which only partial inhibition of migration was achieved, the migration of β_3-null endothelial cells was still significantly greater than wild-type cells ($P < 0.05$). This difference in sensitivity to the inhibitor may be a consequence of the enhanced activation of ERK1/2 that occurs in β_3-null endothelial cells. UO126, albeit at higher concentrations, was also able to inhibit VEGF-induced microvessel growth from wild-type and β_3-null aortic rings in a dose-dependent manner (Fig. 6*B*), and at the nonsaturating dose of 5 μmol/L, sprouting from β_3-null aortic rings was significantly greater than wild-type ($P < 0.05$). Therefore, the increased phosphorylation of ERK1/2 in β_3-null endothelial cells is involved in mediating the enhanced response of these cells to VEGF.

DISCUSSION

We propose that Flk1-mediated responses to VEGF are enhanced in β_3-null mice, leading to augmented angiogenesis and increased tumor growth. Therefore, β_3-integrin could be a negative regulator of VEGF signaling.

Endothelial cell expression of β_3-integrin and Flk1 can be upregulated during angiogenesis, and antagonists of both molecules inhibit pathological angiogenesis in mice, suggesting a role for both molecules in tumor neovascularization (10, 12, 39, 40). Moreover, binding of β_3-integrin to vitronectin enhances the phosphorylation of Flk1 in response to VEGF, suggesting that β_3-integrin can promote Flk1 signaling during angiogenesis (41). However, studies in β_3-integrin–deficient mice show that this integrin is not required for tumor or VEGF-specific angiogenesis (7), and we now show that enhanced Flk1 signaling occurs in endothelial cells in which β_3-integrin is absent.

How does enhanced Flk1 signaling occur as a consequence of β_3 integrin deficiency? $\alpha_v\beta_3$ integrin expression in endothelial cells can suppress Flk1 expression, which results in at least 2-fold elevated cellular levels of Flk1 in β_3-null endothelial cells when compared with wild-type cells (7). In concordance, when β_3-null endothelial cells receive a VEGF stimulus, the amount of phosphorylated Flk1 receptor that results is also 2-fold greater when compared with wild-type cells (Fig. 5). Although we have limited our *in vitro* studies to stimulation with VEGF-A^{164}, it is also possible that the other Flk1 ligands, *i.e.*, VEGF-A^{120}, VEGF-A^{144}, VEGF-A^{188}, VEGF-C, and

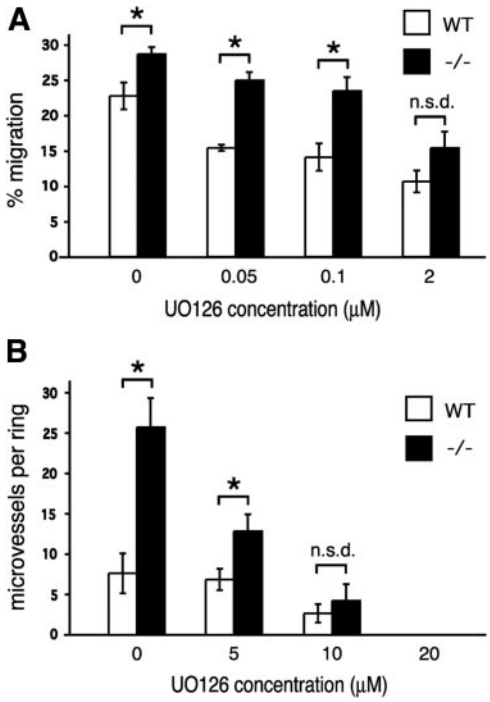

Fig. 6. Enhanced responses to VEGF *in vitro* require signaling through ERK1/2. *A,* quantification of wild-type (*WT*) and β_3-null (−/−) endothelial cell migration in response to VEGF in the presence of MEK inhibitor, UO126. After a 1 hour preincubation with serum-free medium supplemented with varying concentrations of UO126 or vehicle alone, confluent monolayers of wild-type or β_3-null endothelial cells were scratched with a P-200 pipette tip. The medium was replaced with fresh medium containing inhibitors or vehicle and additionally supplemented with 25 ng/mL VEGF before cells were returned to the incubator for an additional 8 hours. *Bars* show percentage migration relative to 0 hours ± *SEM*; ∗, $P < 0.05$; n.s.d., no significant difference. *B,* quantification of microvessels produced by wild-type and β_3-null aortic rings after 6 days in response to VEGF in the presence of varying concentrations of UO126. Wild-type or β_3-null aortic rings were embedded in Matrigel and overlaid with medium supplemented with 2% FCS, 30 ng/mL VEGF, and varying concentrations of UO126 or vehicle alone. Aortic rings were cultured at 37°C with replacement of the medium every 2 days. *Bars* show mean microvessel number per ring ± *SEM*; ∗, $P < 0.05$.

VEGF-D (10, 12), might also elicit the same effect. In any case, the increased activation of Flk1 can lead to enhanced activation of downstream signaling molecules, such as ERK1/2 (Fig. 5) and augmented endothelial cell responses to VEGF, such as enhanced cell migration and proliferation (Fig. 4). Because Flk1 inhibition reduces the enhanced angiogenesis and tumor growth seen in β_3-null mice (Figs. 1–3), enhanced Flk1 signaling may mediate the augmented angiogenesis and tumor growth seen in β_3-null animals *in vivo*. Therefore, β_3 integrin can enhance or inhibit VEGF signaling via different mechanisms: Vitronectin binding to β_3-integrin promotes Flk1 phosphorylation and downstream signaling (41), whereas suppression of Flk1 expression by β_3-integrin limits the total cellular levels of Flk1 available for phosphorylation and downstream signaling.

The 2- to 3-fold increase in Flk1 expression seen in β_3-null endothelial cells (7) results in increased angiogenesis and tumor growth *in vivo*, suggesting that the expression level of Flk1 is a major determinant of angiogenic potential *in vivo*. This is supported by data showing that levels of endothelial Flk1 are spatially and temporally regulated during developmental angiogenesis (27, 40) and increased during pathologic angiogenesis (25, 26). Although beyond the scope of the current study, it would also be interesting to determine whether the levels and activity of other VEGF receptors are altered in β_3-null mice.

Other mechanisms may also contribute to the enhanced angiogenesis seen in β_3-null mice. Firstly, because β_3-integrin binding to vitronectin can enhance Flk1 signaling in response to VEGF (41), β_3-integrin binding to another ligand might attenuate signaling through Flk1, perhaps by enhancing the association of Flk1 with protein tyrosine phosphatases. In β_3-null mice, this signal attenuation mechanism would be absent, leading to enhanced VEGF responses. Secondly, β_3-integrin mediates the growth inhibitory effect of several endogenous inhibitors of angiogenesis, including tumstatin (8, 42–44). Hamano *et al*. (45) showed that tumstatin-deficient mice have enhanced tumor growth and angiogenesis, that β_3-integrin–deficient mice do not respond to tumstatin, and that the presence of β_3-integrin–positive vessels in tumors correlates with tumstatin efficacy. This suggests that the enhanced angiogenesis seen in β_3-null mice may be mediated, at least in part, by a lack of response to tumstatin. Finally, the accumulation of ligand-free β_3-integrin on cells *in vitro* can promote apoptosis via so-called "integrin-mediated death" (46, 47). It was proposed that unligated β_3-integrin drives endothelial cell apoptosis in the tumors of wild-type animals and that this mechanism is absent in β_3-null mice, giving rise to enhanced angiogenesis (46). Given that β_3-integrin probably plays multiple roles in angiogenesis (8, 44, 48, 49), it is possible that these other mechanisms may be operating in parallel with our proposed mechanism.

Integrins and VEGF-mediated signaling may be excellent targets for the anti-angiogenic therapy of human cancer. We are investigating how integrins and their antagonists can influence VEGF signaling. For example, how does β_3-integrin transduce signals that depress the expression of Flk1 and can other integrins function in the same fashion? Understanding this may provide new clues as to how integrins or congruous signaling molecules may be pharmacologically targeted to suppress Flk1 levels and angiogenesis in tumors. Because integrin antagonists have been shown to activate integrin-mediated signaling (8, 50–52), it is possible that integrin antagonists may function by suppressing Flk1 levels or Flk1 signaling. Is β_3-integrin–mediated suppression of Flk1 levels relevant to human tumors? A phase I clinical trial of Vitaxin, a β_3-integrin antagonist, gave variable results in the clinic (6). It was recently reported that only 8 to 40% of mouse tumor blood vessels stain positive for β_3-integrin (45), which may explain why tumors do not respond consistently to Vitaxin. Because our data suggest that β_3-integrin–negative blood vessels may have enhanced Flk1 signaling, an effective means to target both β_3-integrin–negative and –positive blood vessels may be to combine β_3-integrin antagonists with Flk1 antagonists *in vivo*.

ACKNOWLEDGMENTS

We thank Garry Saunders, Sue Watling, and Colin Wren for their assistance with experiments; Ian Hart and Richard Hynes for their criticism of the work; and Fiona Parkinson for her help in the manuscript preparation.

REFERENCES

1. Hanahan D, Folkman J. Patterns and emerging mechanisms of the angiogenic switch during tumorigenesis. Cell 1996;86:353–64.
2. Brooks PC, Clark RA, Cheresh DA. Requirement of vascular integrin $\alpha v\beta 3$ for angiogenesis. Science 1994;2645:69–71.
3. Brooks PC, Montgomery AM, Rosenfeld M, et al. Integrin $\alpha v\beta 3$ antagonists promote tumor regression by inducing apoptosis of angiogenic blood vessels. Cell 1994;791: 157–64.
4. Friedlander M, Brooks PC, Shaffer RW, Kincaid CM, Varner JA, Cheresh DA. Definition of two angiogenic pathways by distinct αv integrins. Science 1995;270: 1500–2.
5. Friedlander M, Theesfeld CL, Sugita M, et al. Involvement of integrins $\alpha v\beta 3$ and $\alpha v\beta 5$ in ocular neovascular diseases. Proc Natl Acad Sci USA 1996;93:9764–9.
6. Gutheil JC, Campbell TN, Pierce PR, et al. Targeted antiangiogenic therapy for cancer using Vitaxin: a humanized monoclonal antibody to the integrin $\alpha_v\beta_3$. Clin Cancer Res 2000;6:3056–61.
7. Reynolds LE, Wyder L, Lively JC, et al. Enhanced pathological angiogenesis in mice lacking $\beta 3$ integrin or $\beta 3$ and $\beta 5$ integrins. Nat Med 2002;8:27–34.
8. Hynes RO. A reevaluation of integrins as regulators of angiogenesis. Nat Med 2002;8:918–21.

9. Kerbel R, Folkman J. Clinical translation of angiogenesis inhibitors. Nat Rev Cancer 2002;2:727–39.
10. Neufeld G, Cohen T, Gengrinovitch S, Poltorak Z. Vascular endothelial growth factor (VEGF) and its receptors. FASEB J 1999;13:9–22.
11. Carmeliet P. Mechanisms of angiogenesis and arteriogenesis. Nat Med 2000;6: 389–95.
12. Matsumoto T, Claesson-Welsh L. VEGF receptor signal transduction. Sci STKE 2001. Dec 11;(112) RE21. http://stke.sciencemag.org/cgi/content/full/OC_sigtrans; 2001/112/re21.
13. Meyer M, Clauss M, Lepple-Wienhues A, et al. A novel vascular endothelial growth factor encoded by Orf virus, VEGF-E, mediates angiogenesis via signalling through VEGFR-2 (KDR) but not VEGFR-1 (Flt-1) receptor tyrosine kinases. EMBO J 1999;18:363–74.
14. Gille H, Kowalski J, Li B, et al. Analysis of biological effects and signaling properties of Flt-1 (VEGFR-1) and KDR (VEGFR-2): A reassessment using novel receptor-specific vascular endothelial growth factor mutants. J Biol Chem 2001;276:3222–30.
15. Hiratsuka S, Minowa O, Kuno J, et al. Flt-1 lacking the tyrosine kinase domain is sufficient for normal development and angiogenesis in mice. Proc Natl Acad Sci USA 1998;95:9349–54.
16. Autiero M, Waltenberger J, Communi D, et al. Role of PlGF in the intra- and intermolecular cross talk between the VEGF receptors Flt1 and Flk1. Nat Med 2003;9:936–43.
17. Luttun A, Autiero M, Tjwa M, et al. Genetic dissection of tumor angiogenesis: are PlGF and VEGFR-1 novel anti-cancer targets? Biochim Biophys Acta 2004;1654: 79–94.
18. Soker S, Takashima S, Miao HQ, Neufeld G, Klagsbrun M. Neuropilin-1 is expressed by endothelial and tumor cells as an isoform-specific receptor for vascular endothelial growth factor. Cell 1998;92:735–45.
19. Soker S, Miao HQ, Nomi M, Takashima S, Klagsbrun M. VEGF165 mediates formation of complexes containing VEGFR-2 and neuropilin-1 that enhance VEGF165-receptor binding. J Cell Biochem 2002;85:357–68.
20. Miao HQ, Soker S, Feiner L, Alonso JL, Raper JA, Klagsbrun M. Neuropilin-1 mediates collapsin-1/semaphorin III inhibition of endothelial cell motility: functional competition of collapsin-1 and vascular endothelial growth factor-165. J Cell Biol 1999;146:233–42.
21. Kessler O, Shraga-Heled N, Lange T, et al. Semaphorin-3F is an inhibitor of tumor angiogenesis. Cancer Res 2004;64:1008–15.
22. Kroll J, Waltenberger J. The vascular endothelial growth factor receptor KDR activates multiple signal transduction pathways in porcine aortic endothelial cells. J Biol Chem 1997;272:32521–7.
23. Hood JD, Frausto R, Kiosses WB, Schwartz MA, Cheresh DA. Differential αv integrin-mediated Ras-ERK signaling during two pathways of angiogenesis. J Cell Biol 2003;162:933–43.
24. Eliceiri BP, Klemke R, Stromblad S Cheresh DA. Integrin $\alpha v\beta 3$ requirement for sustained mitogen-activated protein kinase activity during angiogenesis. J Cell Biol 1998;140:1255–6.
25. Plate KH, Breier G, Millauer B, Ullrich A, Risau W. Up-regulation of vascular endothelial growth factor and its cognate receptors in a rat glioma model of tumor angiogenesis. Cancer Res 1993;53:5822–7.
26. Brown LF, Berse B, Jackman RW, et al. Increased expression of vascular permeability factor (vascular endothelial growth factor) and its receptors in kidney and bladder carcinomas. Am J Pathol 1993;143:1255–62.
27. Gerhardt H, Golding M, Fruttiger M, et al. VEGF guides angiogenic sprouting utilizing endothelial tip cell filopodia. J Cell Biol 161:1163–77.
28. Prewett M, Huber J, Li Y, et al. Antivascular endothelial growth factor receptor (fetal liver kinase 1) monoclonal antibody inhibits tumor angiogenesis and growth of several mouse and human tumors. Cancer Res 1999;59:5209–18.
29. Klement G, Huang P, Mayer B, et al. Differences in therapeutic indexes of combination metronomic chemotherapy and an anti-VEGFR-2 antibody in multidrug-resistant human breast cancer xenografts. Clin Cancer Res 2002;8:221–32.
30. Bruns CJ, Shrader M, Harbison MT, et al. Effect of the vascular endothelial growth factor receptor-2 antibody DC101 plus gemcitabine on growth, metastasis and angiogenesis of human pancreatic cancer growing orthotopically in nude mice. Int J Cancer 2002;102:101–8.
31. Ferrara N, Hillan KJ, Gerber HP, Novotny W. Discovery and development of bevacizumab, an anti-VEGF antibody for treating cancer. Nat Rev Drug Discov 2003;3:391–400.
32. Fong TA, Shawver LK, Sun L, et al. SU5416 is a potent and selective inhibitor of the vascular endothelial growth factor receptor (Flk-1/KDR) that inhibits tyrosine kinase catalysis, tumor vascularization, and growth of multiple tumor types. Cancer Res 1999;59:99–106.
33. Fidler IJ. Selection of successive tumour lines for metastasis. Nat New Biol 1973; 242:148–9.
34. Layton MG, Franks LM. Selective suppression of metastasis but not tumorigenicity of a mouse lung carcinoma by cell hybridization. Int J Cancer 1986;37:723–30.
35. Tille JC, Wang X, Lipson KE, et al. Vascular endothelial growth factor (VEGF) receptor-2 signaling mediates VEGF-C(δNδC)- and VEGF-A-induced angiogenesis *in vitro.* Exp Cell Res 2003;285:286–98.
36. Jat PS, Noble MD, Ataliotis P, et al. Direct derivation of conditionally immortal cell lines from an H-2Kb-tsA58 transgenic mouse. Proc Natl Acad Sci USA 1991;88: 5096–100.
37. Lidington EA, Rao RM, Marelli-Berg FM, Jat PS, Haskard DO, Mason JC. Conditional immortalization of growth factor-responsive cardiac endothelial cells from H-2K(b)-tsA58 mice. Am J Physiol Cell Physiol 2002;282:C67–74.
38. Gerber HP, Malik AK, Solar GP, et al. VEGF regulates haematopoietic stem cell survival by an internal autocrine loop mechanism. Nature 2002;417:954–8.
39. Eliceiri BP, Cheresh DA. The role of αv integrins during angiogenesis: insights into potential mechanisms of action and clinical development. J Clin Investig 1999;103: 1227–30.
40. Millauer B, Wizigmann-Voos S, Schnurch H, et al. High affinity VEGF binding and developmental expression suggest Flk-1 as a major regulator of vasculogenesis and angiogenesis. Cell 1993;72:835–46.
41. Soldi R, Mitola S, Strasly M, Defilippi P, Tarone G, Bussolino F. Role of $\alpha v\beta 3$ integrin in the activation of vascular endothelial growth factor receptor-2. EMBO J 1999;18:882–92.
42. Lawler J. The functions of thrombospondin-1 and -2. Curr Opin Cell Biol 2000;12: 634–40.
43. Maeshima Y, Sudhakar A, Lively JC, et al. Tumstatin, an endothelial cell-specific inhibitor of protein synthesis. Science 2002;295:140–3.
44. Hodivala-Dilke KM, Reynolds AR, Reynolds LE. Integrins in angiogenesis: multitalented molecules in a balancing act. Cell Tissue Res 2003;314:131–44.
45. Hamano Y, Zeisberg M, Sugimoto H, et al. Physiological levels of tumstatin, a fragment of collagen IV α3 chain, are generated by MMP-9 proteolysis and suppress angiogenesis via $\alpha v\beta 3$ integrin. Cancer Cell 2003;3:589–601.
46. Cheresh DA, Stupack DG. Integrin-mediated death: an explanation of the integrin-knockout phenotype? Nat Med 2002;8:193–4.
47. Stupack DG, Puente XS, Boutsaboualoy S, Storgard CM, Cheresh DA. Apoptosis of adherent cells by recruitment of caspase-8 to unligated integrins. J Cell Biol 2001; 155:459–70.
48. Smyth SS, Patterson C. Tiny dancers: the integrin-growth factor nexus in angiogenic signaling. J Cell Biol 2002;158:17–21.
49. Ruegg C, Dormond O, Mariotti A. Endothelial cell integrins and COX-2: mediators and therapeutic targets of tumor angiogenesis. Biochim Biophys Acta 2004;1654: 51–67.
50. Diaz-Gonzalez F, Forsyth J, Steiner B, Ginsberg MH. Trans-dominant inhibition of integrin function. Mol Biol Cell 1996;7:1939–51.
51. Legler DF, Wiedle G, Ross FP, Imhof BA. Superactivation of integrin $\alpha v\beta 3$ by low antagonist concentrations. J Cell Sci 2001;114:1545–53.
52. Peter K, Schwarz M, Nordt T, Bode C. Intrinsic activating properties of GP IIb/IIIa blockers. Thromb Res 2001;103(Suppl 1):S21–7.